

Accepted Manuscript

Continuous hot-wire chemical vapor deposition on moving glass substrates

A. Bink, M. Brinza, J.P.H. Jongen, R.E.I. Schropp

PII: S0040-6090(09)00053-4
DOI: doi: [10.1016/j.tsf.2009.01.068](https://doi.org/10.1016/j.tsf.2009.01.068)
Reference: TSF 25536

To appear in: *Thin Solid Films*



Please cite this article as: A. Bink, M. Brinza, J.P.H. Jongen, R.E.I. Schropp, Continuous hot-wire chemical vapor deposition on moving glass substrates, *Thin Solid Films* (2009), doi: [10.1016/j.tsf.2009.01.068](https://doi.org/10.1016/j.tsf.2009.01.068)

This is a PDF file of an unedited manuscript that has been accepted for publication. As a service to our customers we are providing this early version of the manuscript. The manuscript will undergo copyediting, typesetting, and review of the resulting proof before it is published in its final form. Please note that during the production process errors may be discovered which could affect the content, and all legal disclaimers that apply to the journal pertain.

Continuous hot-wire chemical vapor deposition on moving glass substrates

A. Bink, M. Brinza, J.P.H. Jongen, and R.E.I. Schropp*

Utrecht University, Faculty of Science, Department of Physics and Astronomy,
Nanophotonics - Physics of Devices, P.O. Box 80.000, 3508 TA Utrecht, the Netherlands.

*presenting and corresponding author: R.E.I.Schropp@uu.nl

ABSTRACT

Hot Wire Chemical Vapor Deposition (HWCVD) is a very suitable technique for homogeneous deposition of thin films on continuously moving substrates in an in-line manufacturing system. This process is further aided by the fact that transport of insulating substrates (such as glass) during deposition can be easily arranged as the substrate is not part of the decomposition mechanism as in plasma enhanced CVD. Rigorous grounding of the moving substrates is not required, and no special care needs to be taken to make shields or liners equipotential planes. Moreover, as the creation of dust particles in the gas phase can be avoided, deposition has been undertaken with the substrates facing upward, thus further simplifying the mounting of the substrates. Amorphous as well as microcrystalline silicon thin films with device-quality properties have been achieved on moving substrates. The first p-i-n solar cells made with a 300-nm thick i-layer that was deposited on a linearly moving substrate already showed efficiencies of 6.4%, despite two air breaks that were needed in these tests.

Keywords: hot wire CVD, continuous in-line deposition, amorphous and microcrystalline silicon, device quality

1. Introduction

In hot-wire chemical vapour deposition (HWCVD) the reactive radicals are created by the catalytic decomposition of source gases at transition metal wires. A number of companies (primarily in Japan) have earlier undertaken the scaling up of the HWCVD method to glass substrates with a larger area [1]. These tests, as far as we know, were all done on stationary substrates, except for the deposition of $\text{SiN}_x\text{:H}$ at Ishikawa Seisakusho, which is on a moving PET foil.

If the hot catalytic filaments are long and straight, the radical source can be regarded as a linear source. If the (colder) ends of the linear source are sufficiently far from the outer edges of the substrate, the source is uniform over the entire width of the substrate. This process is further aided by the fact that transport of insulating substrates (such as glass) during deposition can be easily arranged as the substrate is not part of the decomposition mechanism as in plasma enhanced CVD. Rigorous grounding of the moving substrates is not required, and no special care needs to be taken to make shields or liners equipotential planes. This aspect also enhances the ease of cleaning and maintenance, since HWCVD facilitates the use of disposable liners.

These features make HWCVD a very suitable technique for homogeneous deposition of thin films on continuously moving substrates in an in-line manufacturing system or in a roll-to-roll system. We have earlier precluded to this perspective in ref. 2.

At Utrecht Solar Energy Laboratory (USEL), we have conducted preliminary investigations on the feasibility of performing a HWCVD process uniformly on *moving* Corning 2000 glass (for opto-electronical characterization) and TCO-coated glass substrates (for solar cell fabrication). As the creation of charged dust particles in the gas phase is avoided in HWCVD, deposition has

been undertaken with the substrates facing *upward*, thus further simplifying the mounting of the substrates.

2. Experiment

The deposition experiments have been conducted in our PILOT system (Fig. 1), a two-chamber plus load lock system, originally designed by MVSystems, Inc. (Golden, Colorado), to produce homogeneous thin film silicon layers on a 30 cm x 40 cm substrate using plasma enhanced chemical vapor deposition (PECVD). One chamber is dedicated to n-type and p-type doped layers, the other chamber is used for deposition of intrinsic silicon only, in order to avoid unintentional cross-contamination. The transport system utilizes rails to guide the substrate holder to which the substrates are mounted while moving between chambers or within one of the chambers. The holder can be pushed or pulled along the rail system by a transport arm, thus allowing moving substrates *during* deposition to mimic in-line manufacturing. The PILOT system is also intensively used for the optimization of so called HIT cells (silicon wafer Heterojunction cells with Intrinsic Thin passivating layers; also called SHJ cells – silicon heterojunction cells).

The “intrinsic” chamber (or i-chamber) was adapted by Utrecht University to accommodate a hot-wire assembly without the need to remove the rf electrode. For the purpose of hot-wire deposition, multiple, parallel, 99.9 % pure Ta filaments with a diameter of 0.50 mm are mounted above the substrate transport system and deposition is downward. This is a feasible approach, as the HWCVD process is without the risk of formation of charged particles as there is no plasma that can trap negative species. Above the filament assembly, a shower head gas supply is mounted to achieve an evenly distributed feedstock gas flow.

3. Results

Figure 2 shows an amorphous silicon thin film deposited on a plain glass substrate while it was moving under the filaments. Figure 3 shows the thickness profile as determined with an X-Y optical transmission technique. In this technique, an X-Y table is used to scan the transmission data over a large area. This table can be used to measure samples up to a size of 30 x 40 cm. The light source is adjusted to a wavelength where R is almost constant. In this situation the transmission of the layer scales with the inverse exponent of the thickness of the layer ($T \propto e^{-d}$, where d is the thickness of the film). With this relation, the relative thickness of the film can be calculated. In order to obtain an absolute thickness profile these data are combined with an absolute thickness measurement (either from an R/T measurement over a broad spectrum or by using a step profilometer). In Figure 3 we see that the thickness is quite uniform. There appears to be a region of higher thickness along the transport direction in the middle of the sample as well as close to the edges of the sample and a reduction in thickness in three of the four corners. We attribute this to a temperature profile of the wires along the length of the wires. It is expected that this can be improved by using a chamber that is much wider than the sample; presently the limited size of the chamber still limits the length of the wires.

The dark and photoconductivity of amorphous silicon on moving glass substrates were $\sigma_d = 8 \cdot 10^{-12} \Omega^{-1}\text{cm}^{-1}$ and $\sigma_{ph} = 1.9 \cdot 10^{-6} \Omega^{-1}\text{cm}^{-1}$ (showing an appropriate photoresponse for solar cell applications, in excess of 10^5) and the dark activation energy, as shown in Fig. 4, was $E_a = 0.92$ eV, which indicates the intrinsic property of this material, since the band gap was measured to amount to 1.85 eV. Microcrystalline silicon on moving glass substrates had dark and

photoconductivities, respectively, of $\sigma_d = 2.2 \cdot 10^{-7} \Omega^{-1}\text{cm}^{-1}$ and $\sigma_{ph} = 4.0 \cdot 10^{-5} \Omega^{-1}\text{cm}^{-1}$ (photoresponse of ~ 200). The dark activation energy was $E_a = 0.6 \text{ eV}$, again indicating a Fermi level position close to mid gap. The Raman crystalline fraction R_c was 0.68 (see Fig. 5). R_c is defined as $(I_{510}+I_{520})/(I_{480}+I_{510}+I_{520})$, where the intensity of the peak at 480 cm^{-1} represents amorphous mode of the transverse optical (TO) scattering mode, and peaks at 510 cm^{-1} and 520 cm^{-1} represent the (nano)crystalline modes.

Stimulated by these encouraging results, we ventured the demonstration of p-i-n solar cells. We used standard Asahi U-type TCO-coated glass substrates. The p- and n-layer were made by (stationary) PECVD. For the intrinsic layers we used the processing conditions for amorphous silicon on moving substrates. Despite the two air breaks that were needed because the PECVD is performed with the substrates facing down while the HWCVD is done with the substrate facing up, the solar cells performed very well already with our first attempt (see Fig. 6).

The efficiency was 6.41%, the short circuit current density J_{sc} was 13.38 mA/cm^2 , the open circuit voltage V_{oc} was 0.69 V, and the fill factor was 0.69. The thickness of the i-layer was $\sim 300 \text{ nm}$. The yield was near 100%. While the V_{oc} is rather low, which could be attributed to the low doping level of the p-layer, the fill factor is unexpectedly high considering the two air breaks. In fact, the FF is higher than for the present standard PECVD reference cells from this system.

4. Conclusions

We have shown that it is relatively straightforward to scale up HWCVD from the $5 \text{ cm} \times 5 \text{ cm}$ lab scale to an intermediate substrate size of $20 \text{ cm} \times 20 \text{ cm}$. In the scaled up HWCVD mode, we implemented deposition of device-quality amorphous and microcrystalline silicon on moving substrates, thus showing that in-line manufacturing on moving glass substrates is perfectly

feasible. Therefore, homogeneous deposition on a moving web in a roll to roll mode should also be straightforward. It was shown that both amorphous silicon (a-Si:H) and microcrystalline (μ c-Si:H) i-layers possess adequate photo- and dark conductivities, activation energies, and crystalline fractions. Preliminary a-Si:H p-i-n cells, 300-nm thick, show an efficiency of 6.4%.

References

- [1] H. Matsumura and K. Ohdaira, *Thin Solid Films* **516** (2008) 537-540.
- [2] H. Li, R.H. Franken, R.L. Stolk, C.H.M. van der Werf, J.K. Rath and R.E.I. Schropp, *Thin Solid Films* **516** (2008) 755-757.

Captions:

Figure 1: The pilot system (PILOT) used for demonstrating HWCVD on moving substrates.

Figure 2: An a-Si:H thin film with device-quality properties made on moving glass substrate (approx. 20 cm x 20 cm; Euro coin for reference).

Figure 3: Thickness profile of a 13 cm x 17 cm device-quality amorphous silicon thin film deposited by HWCVD on plain glass on a moving substrate. The thickness is given as a percentage of the maximum thickness. The transport direction is along the x-axis. The wires are mounted in the y-axis direction.

Figure 4: Arrhenius plot of the dark conductivity as a function of the temperature for an amorphous silicon layer deposited on a moving substrate. The tiny kink in the curve around $1000/T = 3.0$ is a negligible artifact, which might be due to movement of cables or another mechanical event. The activation energy is 0.92 eV.

Figure 5: Raman spectrograph of the microcrystalline layer made on a moving substrate.

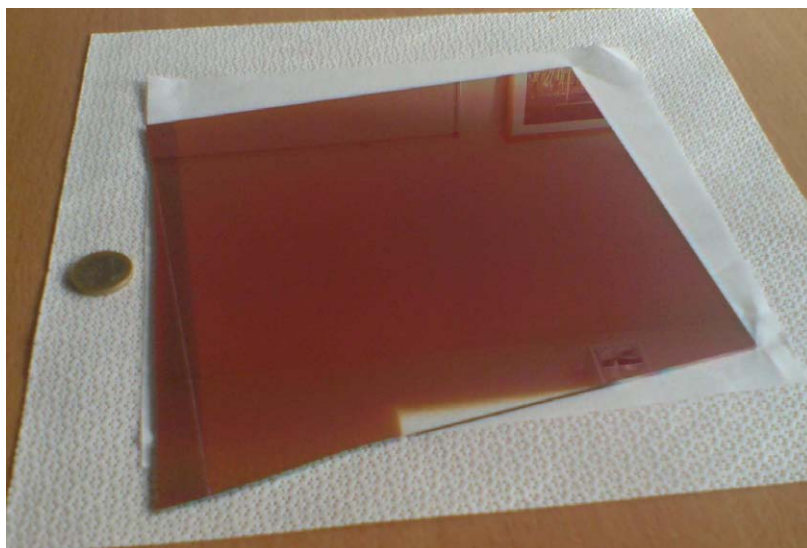
Figure 6: Current density – voltage curve of an a-Si:H p-i-n cell containing an i-layer made by moving-substrate HWCVD. Despite of the two air breaks needed (after the p-layer and after the i-layer) the efficiency is 6.4%, with a FF of 0.692. The performance was measured with a calibrated dual-source AM1.5 solar simulator.

Figure 1:



ACC

Figure 2:



ACCEPTED MANUSCRIPT

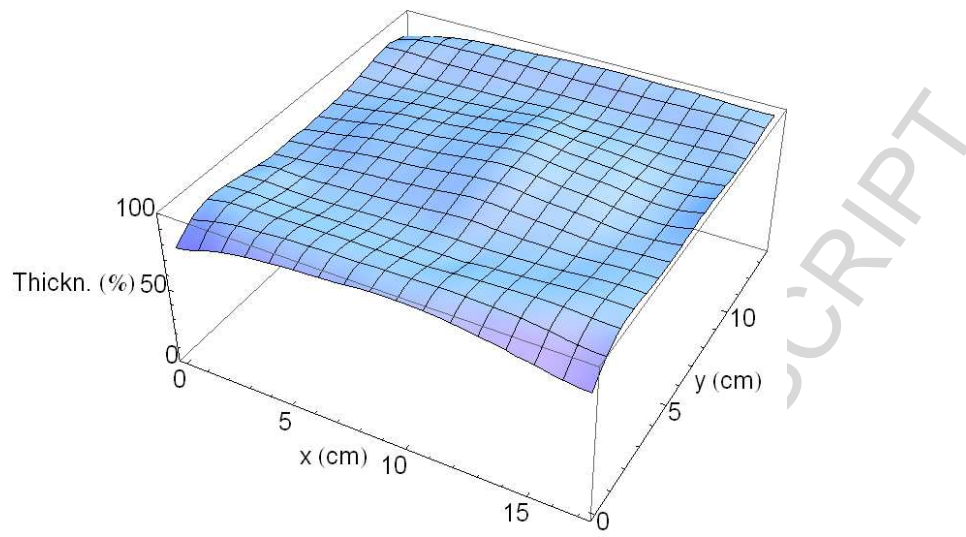
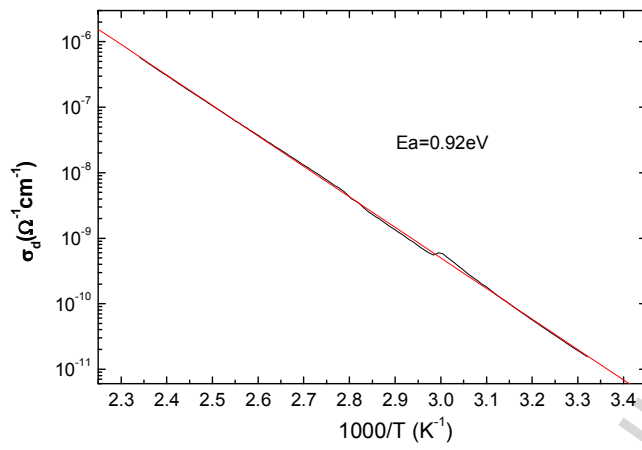
Figure 3:

Figure 4:



ACCEPTED MANUSCRIPT

Figure 5:

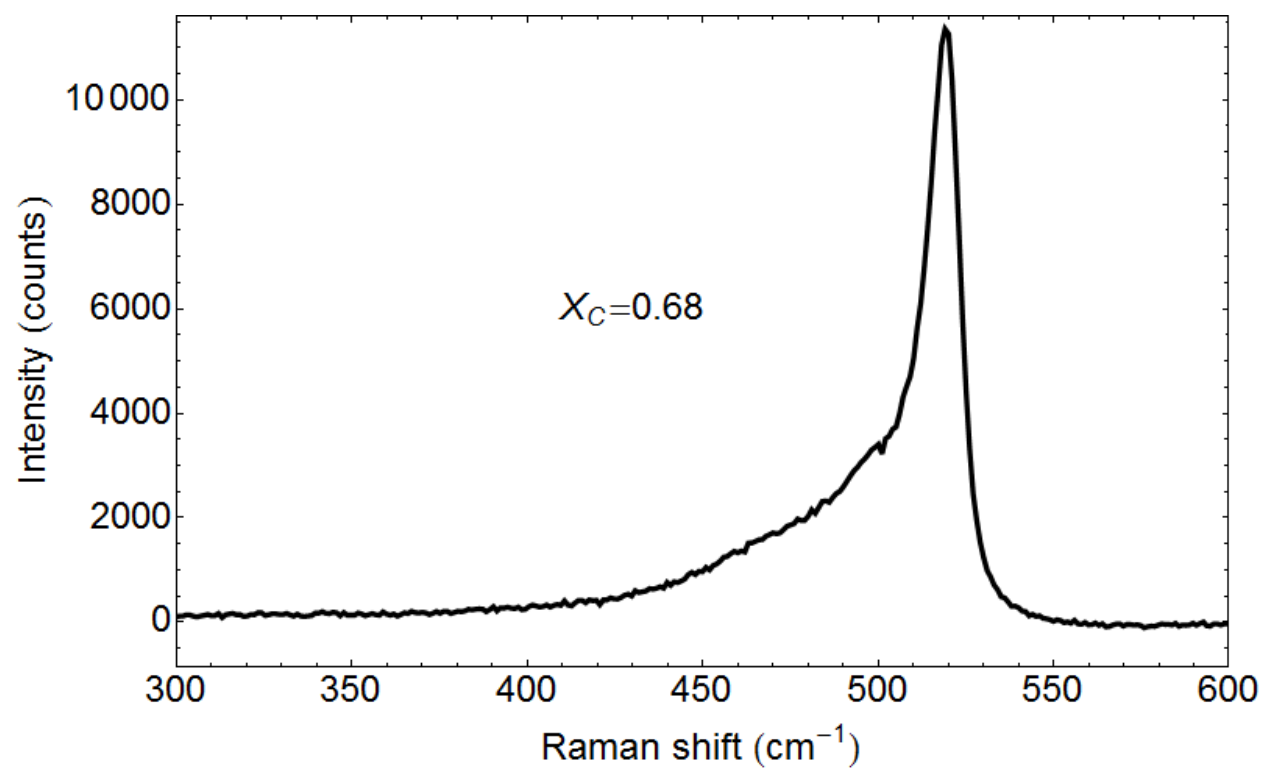
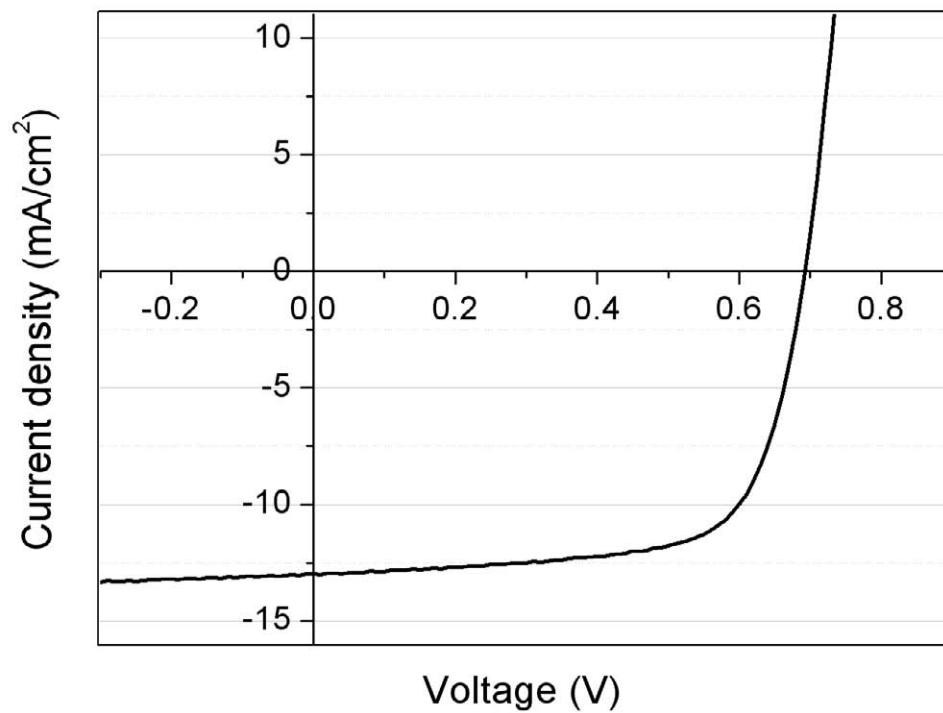


Figure 6:



ACCE